

$\Omega = 13.56$ GHz. This material has very low dispersion at the wavelength of 1.5 microns, so the resonator spectrum around this wavelength is highly equidistant. Light was coupled in and out of the resonator using two optical fibers polished at the optimal coupling angle. The gap between the resonator and the fibers, affecting the light coupling and the resonator loading, was controlled by piezo positioners. The light from the input fiber that did not go into the resonator reflected off of its rim, and was collected by a photodetector. This enabled observation and

measurement of the (absorption) spectrum of the resonator.

The input fiber combined light from two lasers centered at around 1,560 nanometers. Both laser frequencies were simultaneously scanned around the selected WGMs of the same family. However, they were separated by one, two, three, or ten FSRs. This was achieved by fine-tuning each laser frequency offset until the selected resonances overlap on the oscilloscope screen. The resonator quality factor $Q = 7 \times 10^7$ was relatively low to increase the linewidth and, therefore, the duty cycle

of both lasers simultaneously coupled into their WGMs. The optical spectrum analyzer (OSA) connected to the output fiber was continuously acquiring data, asynchronously with the laser scan. The instrument was set to retain the peak power values; therefore, a trace recorded for a sufficiently long period of time reflected the situation with both lasers maximally coupled to the WGMs.

This work was done by Dmitry V. Strekalov and Nan Yu of Caltech and Andrey B. Matsko of OEWaves for NASA's Jet Propulsion Laboratory. Further information is contained in a TSP (see page 1). NPO-46253

Large-Format AlGaN PIN Photodiode Arrays for UV Images

This UV detector can be used for measuring airborne particulates and for biological agent detection.

NASA's Goddard Space Flight Center, Greenbelt, Maryland

A large-format hybridized AlGaN photodiode array with an adjustable bandwidth features stray-light control, ultra-low dark-current noise to reduce cooling requirements, and much higher radiation tolerance than previous technologies. This technology reduces the size, mass, power, and cost of future ultraviolet (UV) detection instruments by using lightweight, low-voltage AlGaN detectors in a hybrid detector/multiplexer configuration. The solar-blind feature eliminates the need for additional visible light rejection and reduces the sensitivity of the system to stray light that can contaminate observations.

The AlGaN UV detector operating at 325 nm gives a 1,000× better extraterrestrial solar radiation rejection than silicon. This reduced need for blocking filters increases the quantum efficiency

(QE) and simplifies the optical systems. The wide direct bandgap reduces the thermally generated dark current to levels that allow many observations at room temperature. Because of this, the AlGaN UV photodiode array doesn't require the extensive cooling (and the associated cooling cost, complexity, and weight) that silicon does, significantly reducing system cost. Wide direct bandgap materials are naturally more radiation tolerant, which is crucial for instruments located outside of Earth's atmosphere.

The device is most sensitive to UV radiation when operated in the photovoltaic mode at or near zero-reverse bias voltage. The effect of the bandgap is seen at the long wavelength cutoff of 365 nm, and shows a contrast ratio before and after the cutoff edge of better than 10^3 . Between 355 and 365 nm, the QE is

fairly flat, with a high of 50 percent at 360 nm at -0.5 V bias. The QE falls rapidly with decreasing wavelength reaching a minimum of 3 percent at 345 nm. The detector's current responsivity at 360 nm and 0 V bias is 0.13 A/W. The spectral detectivity is 2.6×10^{15} cm Hz $^{1/2}$ W $^{-1}$, corresponding to a detector noise equivalent power of 4.1×10^{-18} W/Hz $^{1/2}$.

While the benefits for space-based UV detection are readily apparent, there are Earth-based applications that can benefit as well. These include plume measurements, flame sensing, UV lidar, biological agent detection, and measuring airborne particulate size and velocity.

This work was done by Shahid Aslam and David Franz of Goddard Space Flight Center. Further information is contained in a TSP (see page 1). GSC-15673-1

Fiber-Coupled Planar Light-Wave Circuit for Seed Laser Control in High Spectral Resolution Lidar Systems

The compact, efficient, and reliable design enables use on small aircraft and satellites.

Langley Research Center, Hampton, Virginia

Precise laser remote sensing of aerosol extinction and backscatter in the atmosphere requires a high-power, pulsed, frequency doubled Nd:YAG laser that is wavelength-stabilized to a narrow absorption line such as found in iodine vapor. One method for precise wavelength control is to injection seed the Nd:YAG laser with a

low-power CW laser that is stabilized by frequency converting a fraction of the beam to 532 nm, and to actively frequency-lock it to an iodine vapor absorption line. While the feasibility of this approach has been demonstrated using bulk optics in NASA Langley's Airborne High Spectral Resolution Lidar (HSRL) program, an ideal,

lower cost solution is to develop an all-waveguide, frequency-locked seed laser in a compact, robust package that will withstand the temperature, shock, and vibration levels associated with airborne and space-based remote sensing platforms.

A key technology leading to this miniaturization is the integration of an efficient

waveguide frequency doubling element, and a low-voltage phase modulation element into a single, monolithic, planar light-wave circuit (PLC). The PLC concept advances NASA's future lidar systems due to its compact, efficient and reliable design, thus enabling use on small aircraft and satellites. The immediate application for this technology is targeted for NASA Langley's HSRL system for aerosol and cloud characterization. This Phase I effort proposes the development of a potassium titanyl phosphate (KTP) waveguide phase modulator for future integration into a PLC.

For this innovation, the proposed device is the integration of a waveguide-based frequency doubler and phase modulator in a single, fiber pigtail device that will be capable of efficient second harmonic generation of 1,064- nm light and subsequent phase modulation of the 532 nm light at 250 MHz, providing a properly spectrally formatted beam for HSRL's seed laser locking system. Fabrication of the integrated PLC chip for NASA Langley, planned for the Phase II effort, will require full integration and optimization of the waveguide components (SHG waveguide, splitters,

and phase modulator) onto a single, monolithic device. The PLC will greatly reduce the size and weight, improve electrical-to-optical efficiency, and significantly reduce the cost of NASA Langley's current stabilized HSRL seed laser system built around a commercial off-the-shelf seed laser that is free-space coupled to a bulk doubler and bulk phase modulator.

This work was done by Anthony Cook of Langley Research Center and Shirley McNeil, Gregg Switzer, and Philip Battle of AdvR, Inc. Further information is contained in a TSP (see page 1). LAR-17568-1

On Calculating the Zero-Gravity Surface Figure of a Mirror

As well as gravity reversing between two configurations, mount forces must reverse to within the St. Venant scale.

NASA's Jet Propulsion Laboratory, Pasadena, California

An analysis of the classical method of calculating the zero-gravity surface figure of a mirror from surface-figure measurements in the presence of gravity has led to improved understanding of conditions under which the calculations are valid. In this method, one measures the surface figure in two or more gravity-reversed configurations, then calculates the zero-gravity surface figure as the average of the surface figures determined from these measurements. It is now understood that gravity reversal is not, by itself, sufficient to ensure validity of the calculations: It is also necessary to reverse mounting forces, for which purpose one must ensure that mounting fixture/mirror contacts are located either at the same places or else sufficiently close to the same places in both gravity-reversed configurations. It is usually not practical to locate the contacts at the same places, raising the question of how close is sufficiently close. The criterion for sufficient closeness is embodied in the St. Venant principle, which, in the present context, translates to a requirement that the distance between corresponding gravity-reversed mounting positions be small in comparison to their distances to the optical surface of the mirror.

The necessity of reversing mount forces is apparent in the behavior of the equations familiar from finite element analysis (FEA) that govern deformation of the mirror. In FEA, the three-dimensional solid body (mirror) is approximated by a mesh of N points, and positions of these points, or nodes, are

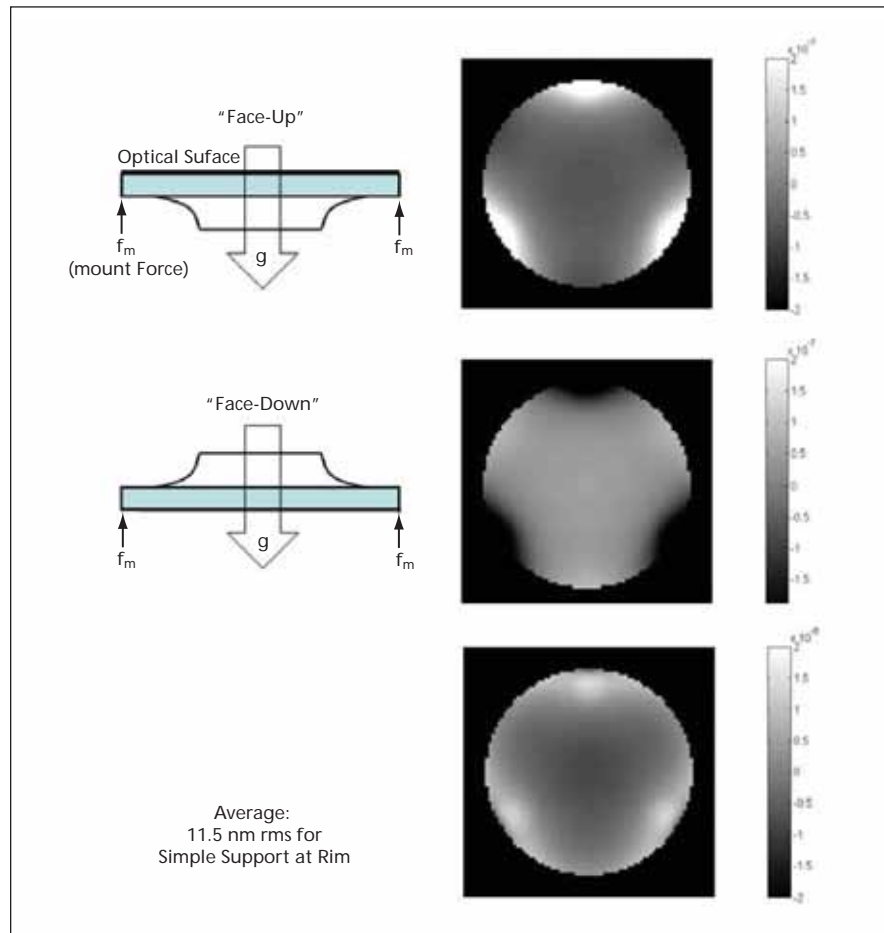


Fig. 1. FEA Modeling of the Surface Figure of PT-M1 during gravity reversal in a simple mirror mount in which the mirror rests on 3 points of contact near the rim (cartoons at left). The mirror model is specified to have a spherical surface in the absence of applied forces. The "face-up" and "face-down" orientations experience gravity forces that are reversed. However, mount forces in the two cases are applied at positions separated by the thickness of the mirror rim, so are only imperfectly reversed. Deformations in the two configurations are shown in the top two panels; their average is shown in the bottom panel, which recovers the ideal spherical surface (which would look flat in this display of departure from sphericity) marred by some dimple artifacts near the rim. The rms error in the average is 11.5 nm.